

Supporting Information for

**Thermodynamically neutral Kubas-type hydrogen storage
using amorphous Cr(III) alkyl hydride gels**

Leah Morris^a, Michel L. Trudeau^b, Daniel Reed^c, David Book^c and David M. Antonelli^{*a}

^a Sustainable Environment Research Centre, University of South Wales, Pontypridd, CF37 4BD, United Kingdom

^b IREQ, Hydro-Quebec, 1800 Boul. Lionel-Boulet, Varennes, Quebec, J3X 1S1, Canada

^c School of Metallurgy and Materials, University of Birmingham, Edgbaston, Birmingham B15 2TT, United Kingdom

Total number of pages: 12

Table of Contents

Figure S1. Infrared spectrum of Cr-100	3
Figure S2. Infrared spectrum of Cr-150C-H ₂	3
Figure S3. Infrared spectrum of Cr-25C-H ₂	4
Figure S4. Nitrogen adsorption (red)-desorption (blue) isotherms of Cr-100	4
Figure S5. Nitrogen adsorption (red)-desorption (blue) isotherms of Cr-25C-H ₂	5
Figure S6. BET transform plot of Cr-100	5
Figure S7. BET transform plot of Cr-25C-H ₂	6
Table T1. Nitrogen adsorption-desorption data	6
Figure S8. PXRD of Cr-100	7
Figure S9. PXRD of Cr-150C-H₂	7
Figure S10. PXRD of Cr-25C-H₂	8
Figure S11. TGA (red) and DTA (purple) curves of Cr-100	8
Figure S12. TGA (red) and DTA (purple) curves of Cr-150C-H ₂	9
Figure S13. TGA (red) and DTA (purple) curves of Cr-25C-H ₂	9
Figure S14. Peak fitting of chromium 2p _{1/2} and 2p _{3/2} region of XPS of Cr-100	10
Figure S15. Baseline corrected peak fitting of chromium 2p _{1/2} and 2p _{3/2} region of XPS of Cr-100	10
Figure S16. Peak fitting of chromium 2p _{1/2} and 2p _{3/2} region of XPS of Cr-150C-H ₂	11
Figure S17. Peak fitting of chromium 2p _{1/2} and 2p _{3/2} region of XPS of Cr-150C-H ₂	11
Figure S18. Peak fitting of chromium 2p _{1/2} and 2p _{3/2} region of XPS of Cr-25C-H ₂	12
Figure S19. Baseline corrected peak fitting of chromium 2p _{1/2} and 2p _{3/2} region of XPS of Cr-25C-H ₂	12

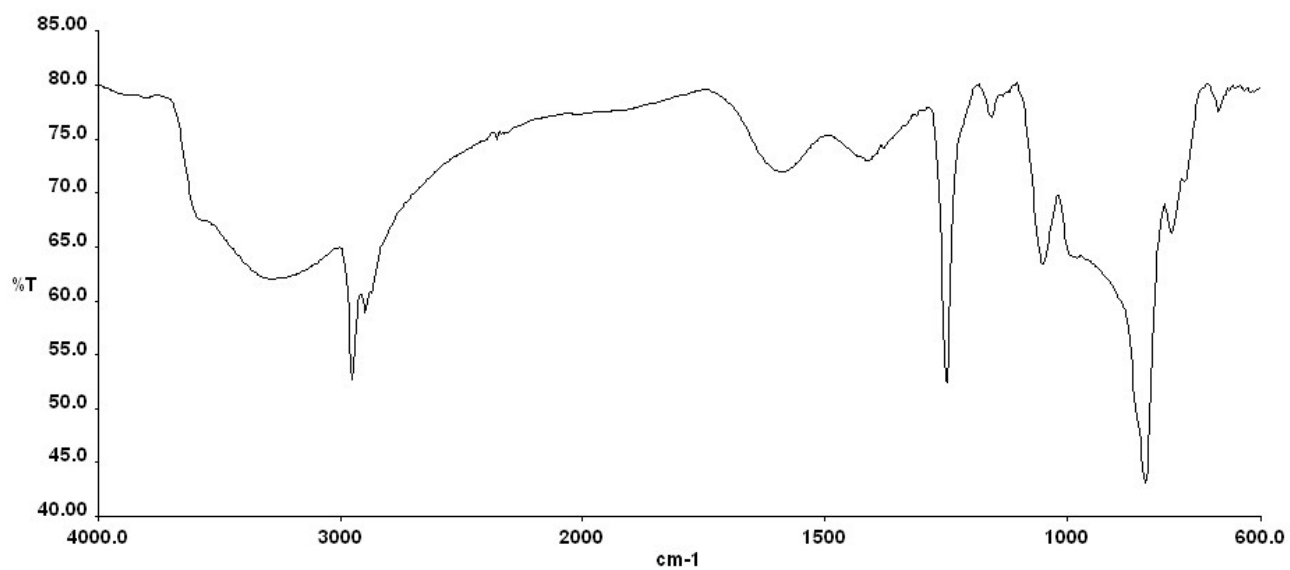


Figure S1. Infrared spectrum of Cr-100

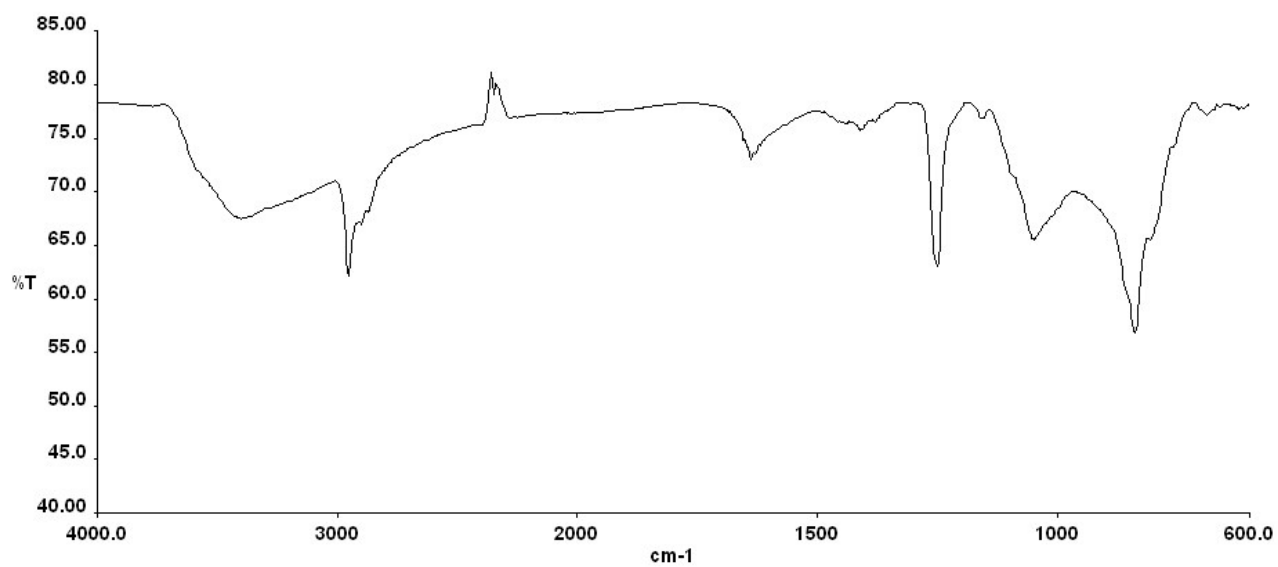


Figure S2. Infrared spectrum of Cr-150C-H₂

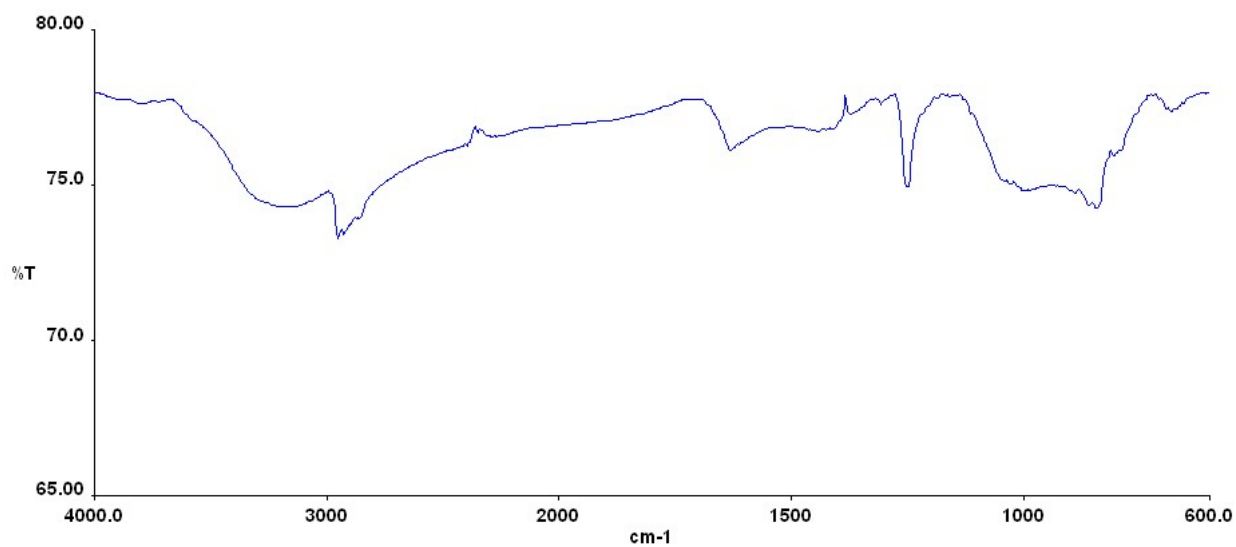


Figure S3. Infrared spectrum of Cr-25C-H₂

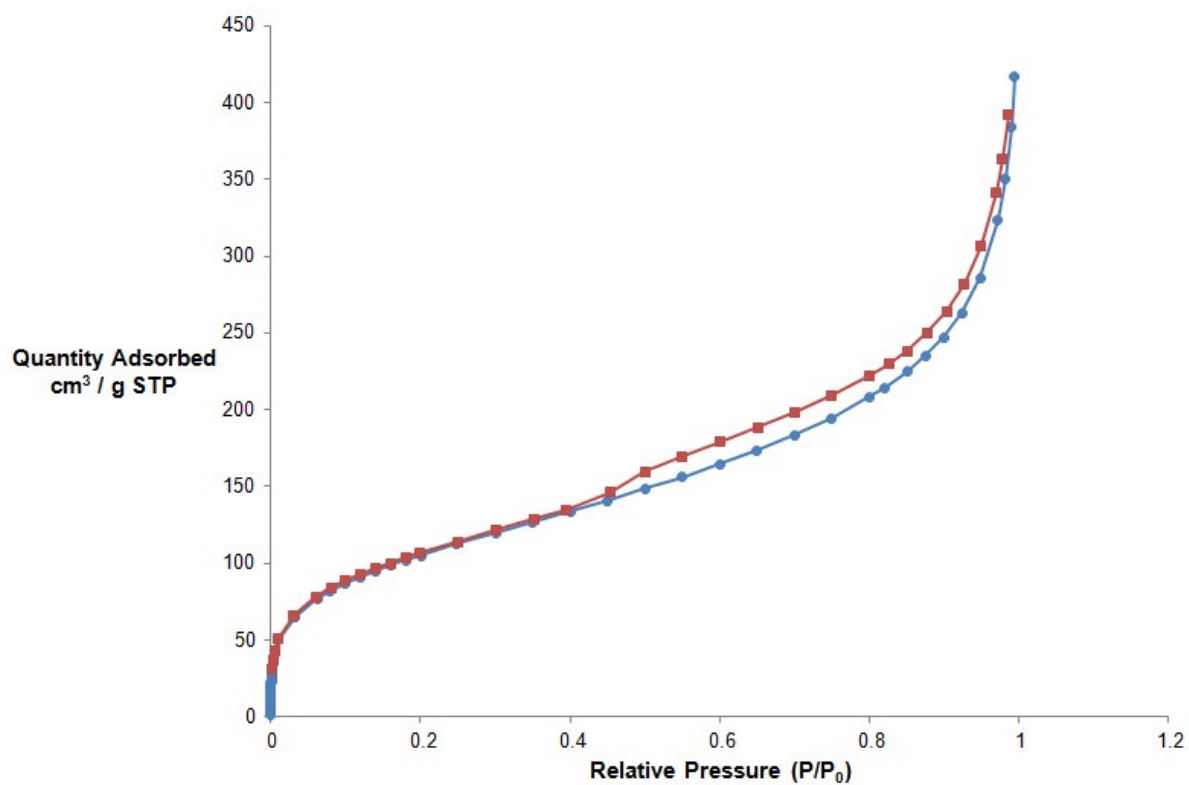


Figure S4. Nitrogen adsorption (red)-desorption (blue) isotherms of Cr-100

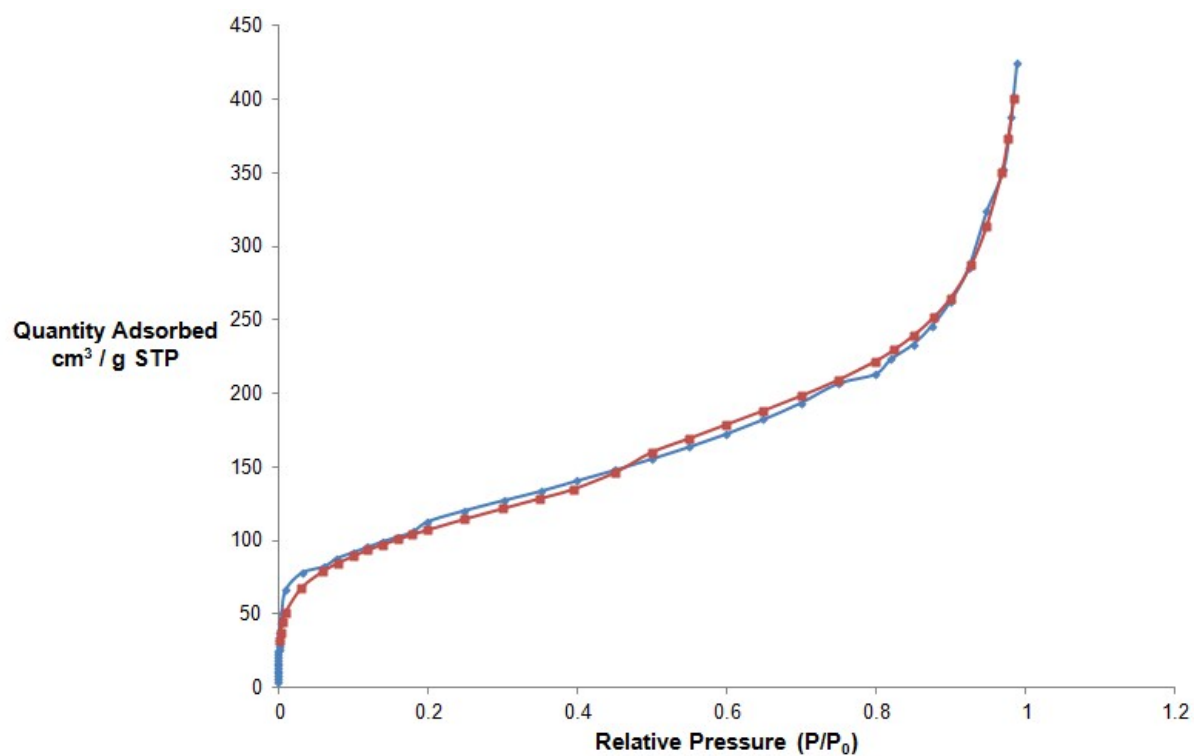


Figure S5. Nitrogen adsorption (red)-desorption (blue) isotherms of Cr-25C-H₂

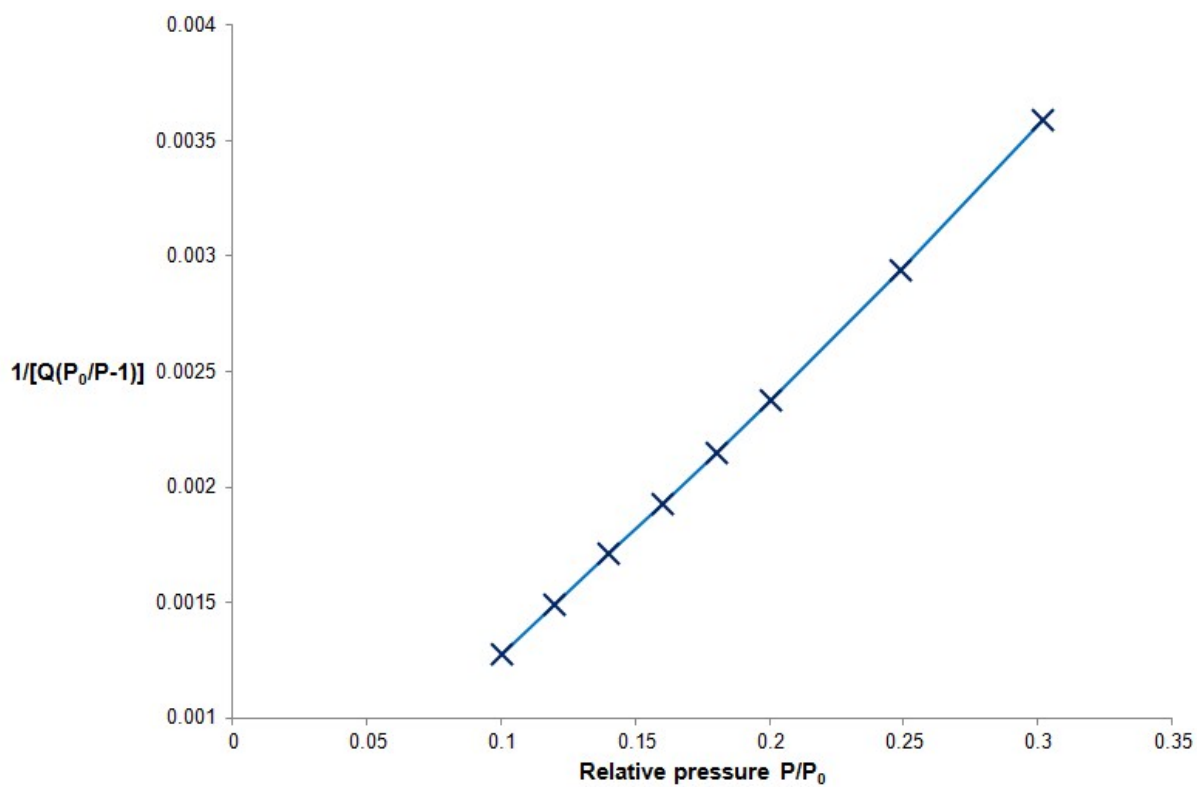


Figure S6. BET transform plot of Cr-100

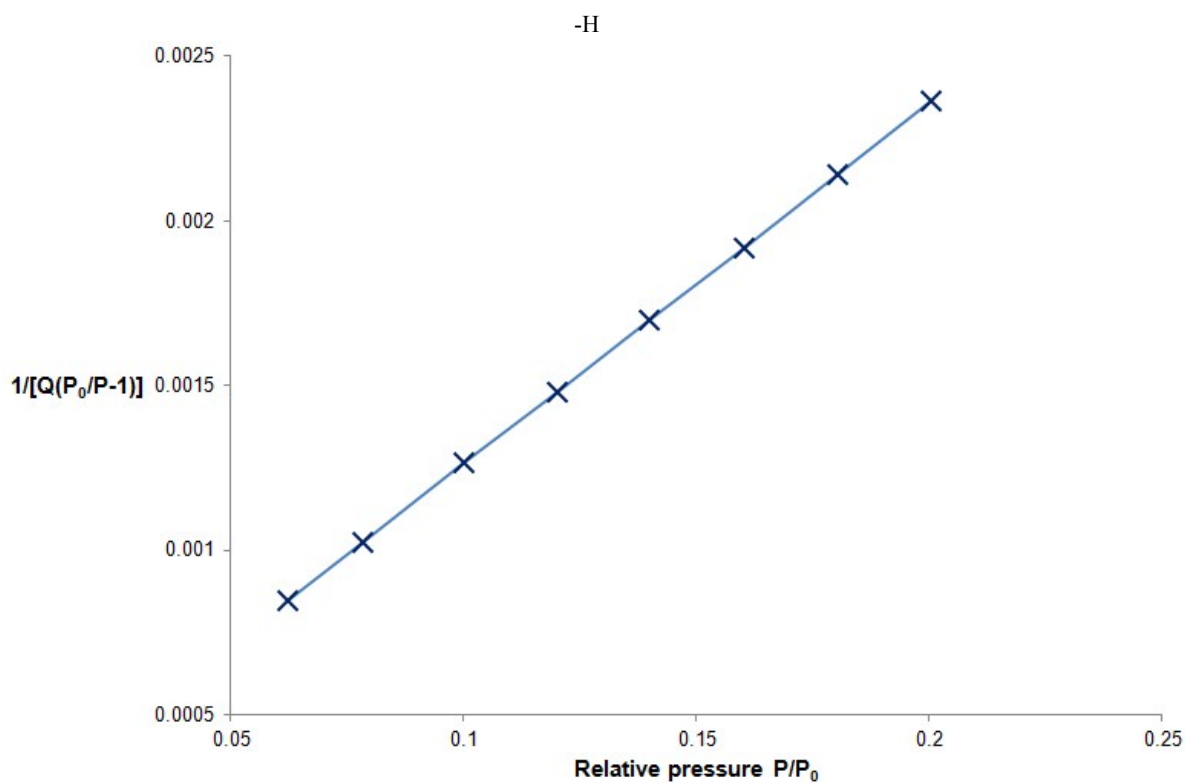


Figure S7. BET transform plot of Cr-25C-H₂

Sample	BET surface area (m ³ /g)	Pore volume (cm ³ /g)	Average BJH desorption pore size (Å)
Cr-100	377	0.218	36.74
Cr-25C-H ₂	391	0.215	36.79

Table T1. Nitrogen adsorption-desorption data

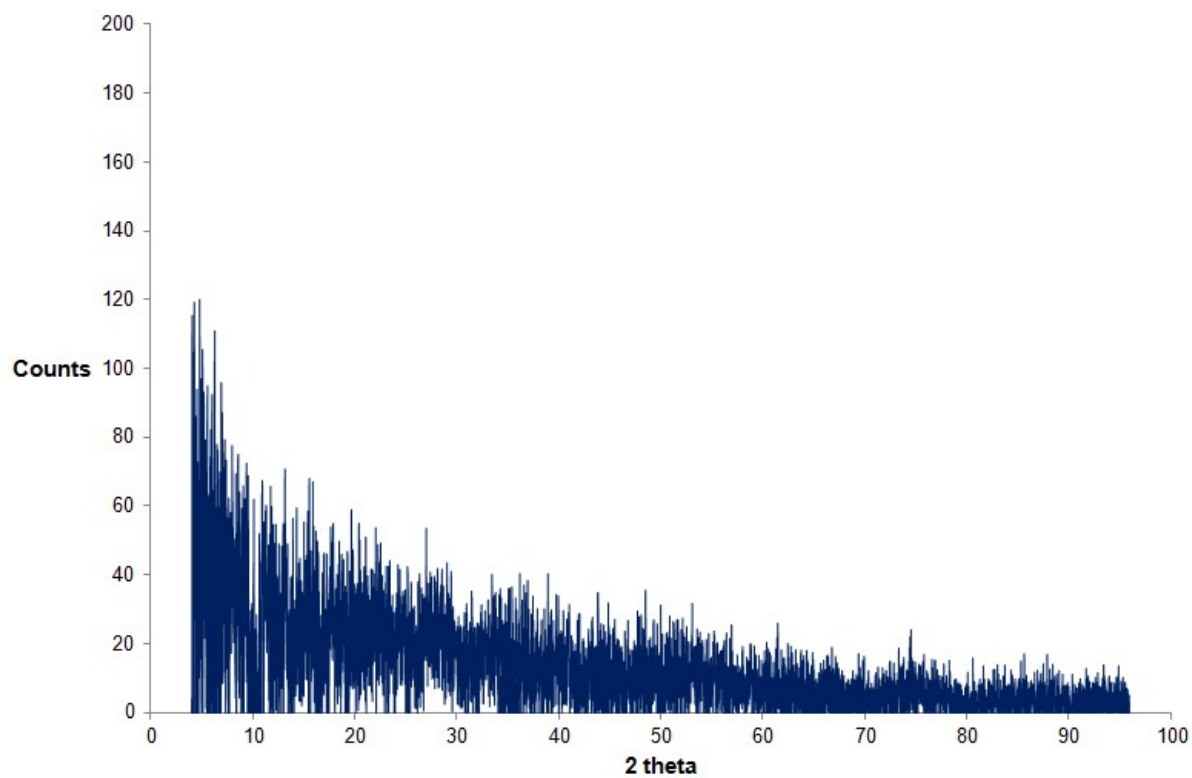


Figure S8. PXRD of Cr-100

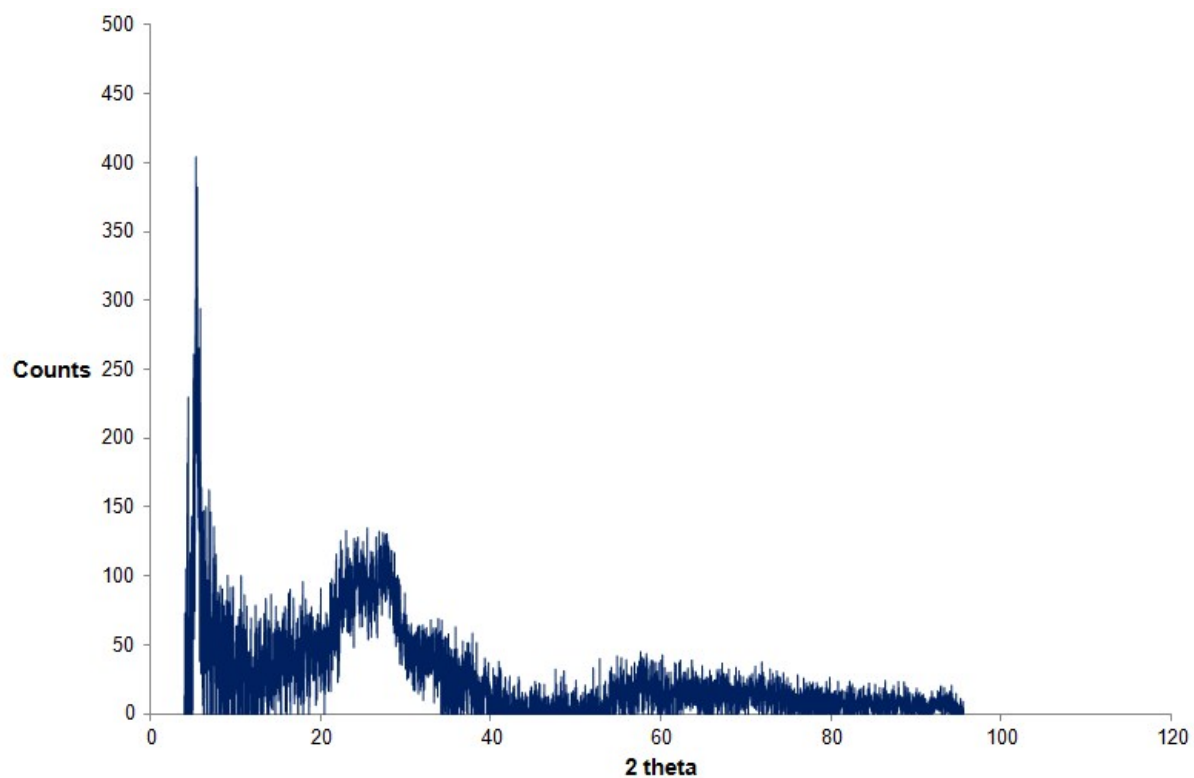


Figure S9. PXRD of Cr-150C-H₂

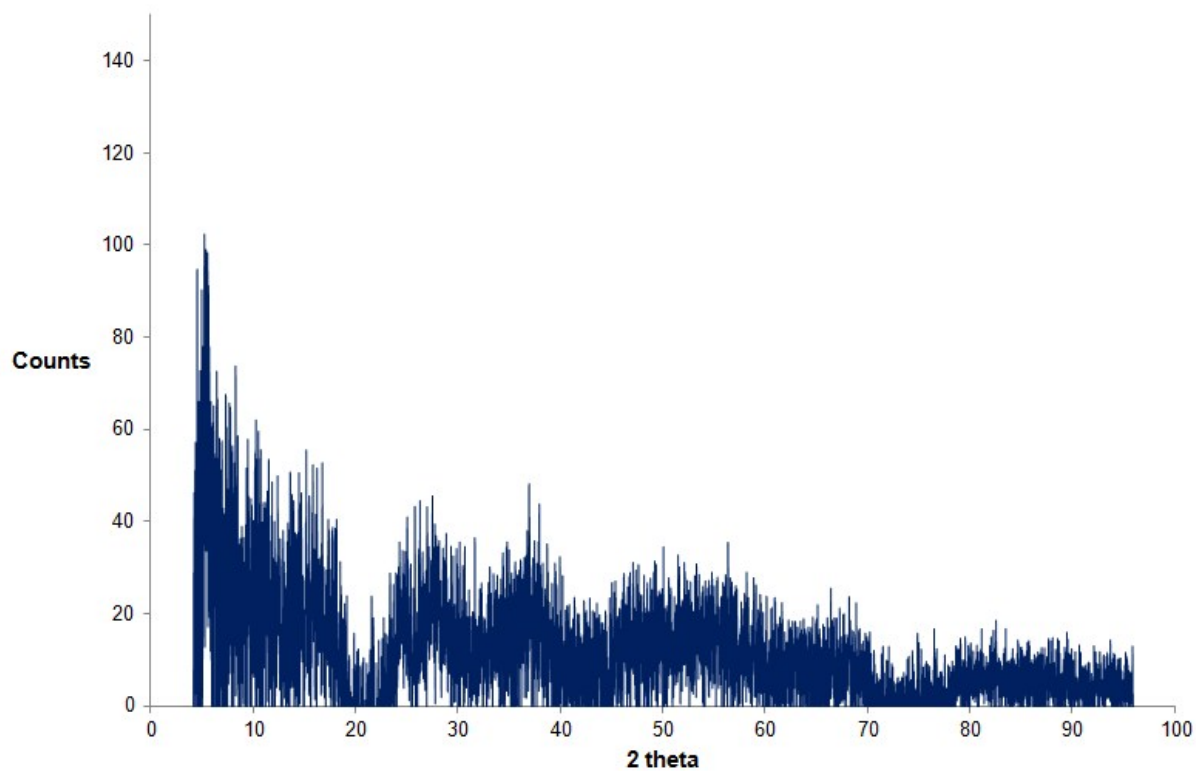


Figure S10. PXRD of Cr-25C-H₂

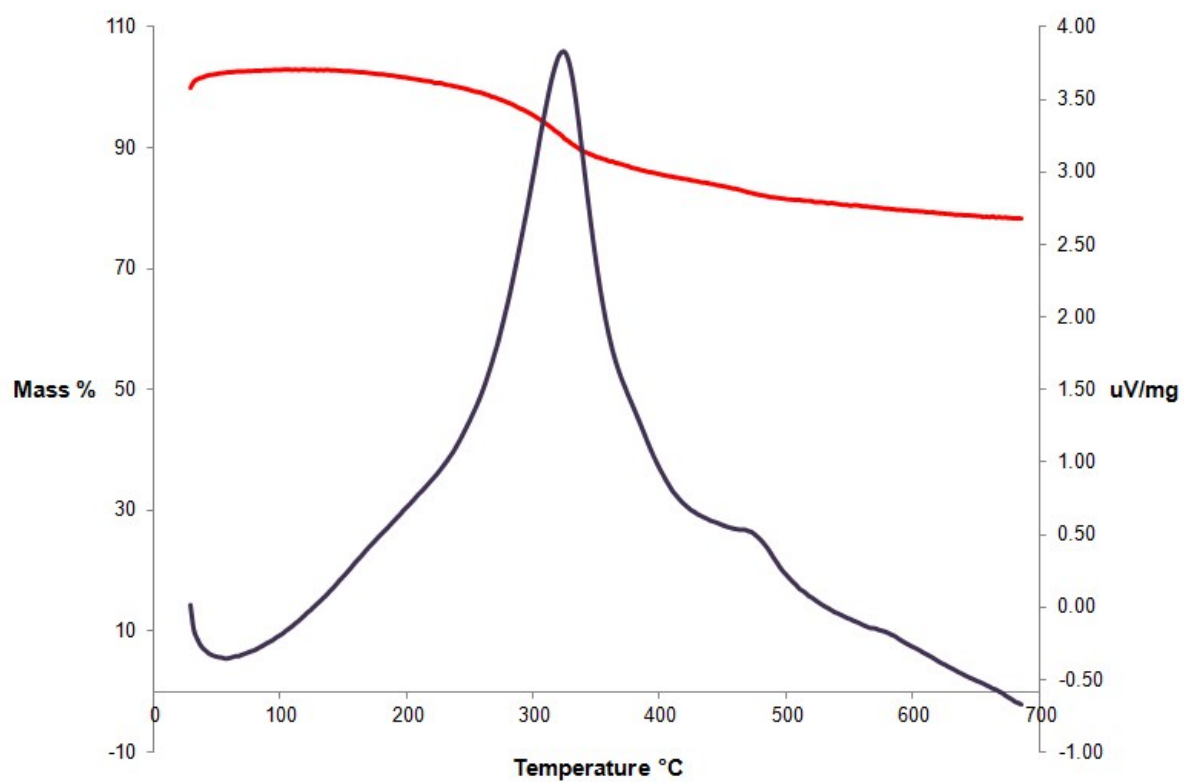


Figure S11. TGA (red) and DTA (purple) curves of Cr-100

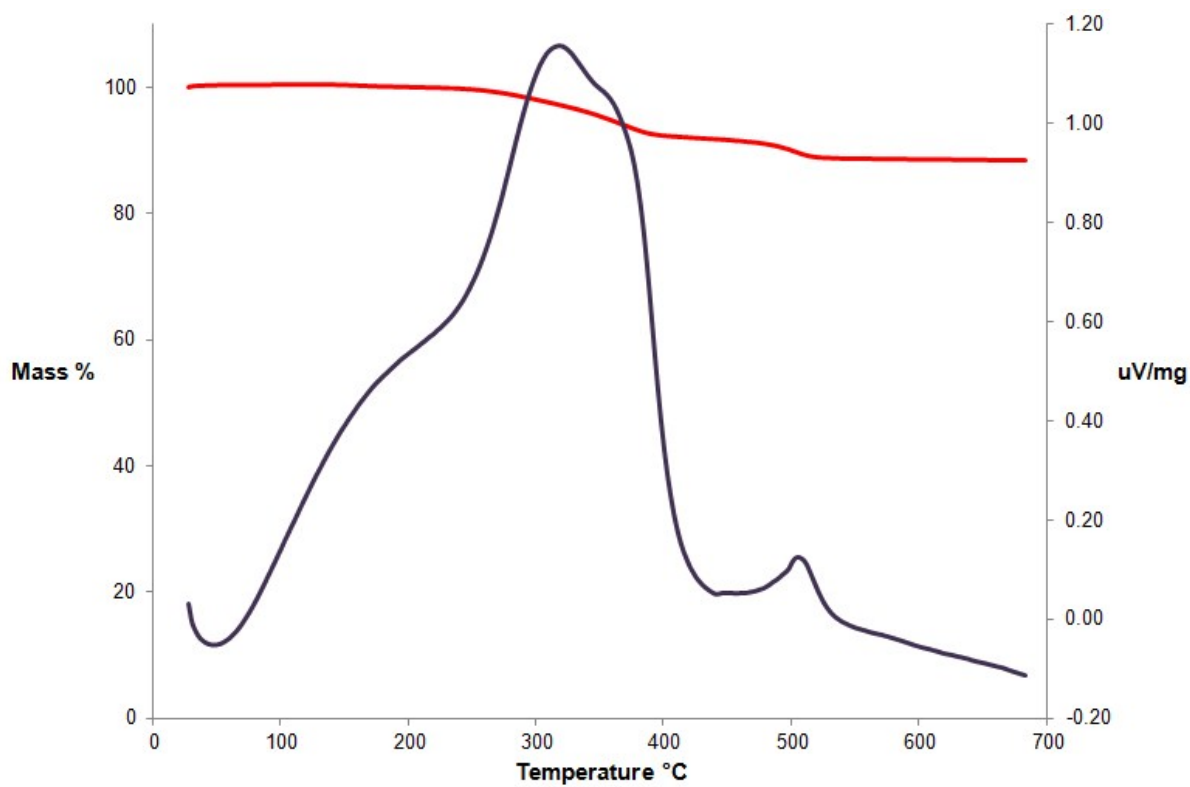


Figure S12. TGA (red) and DTA (purple) curves of Cr-150C-H₂

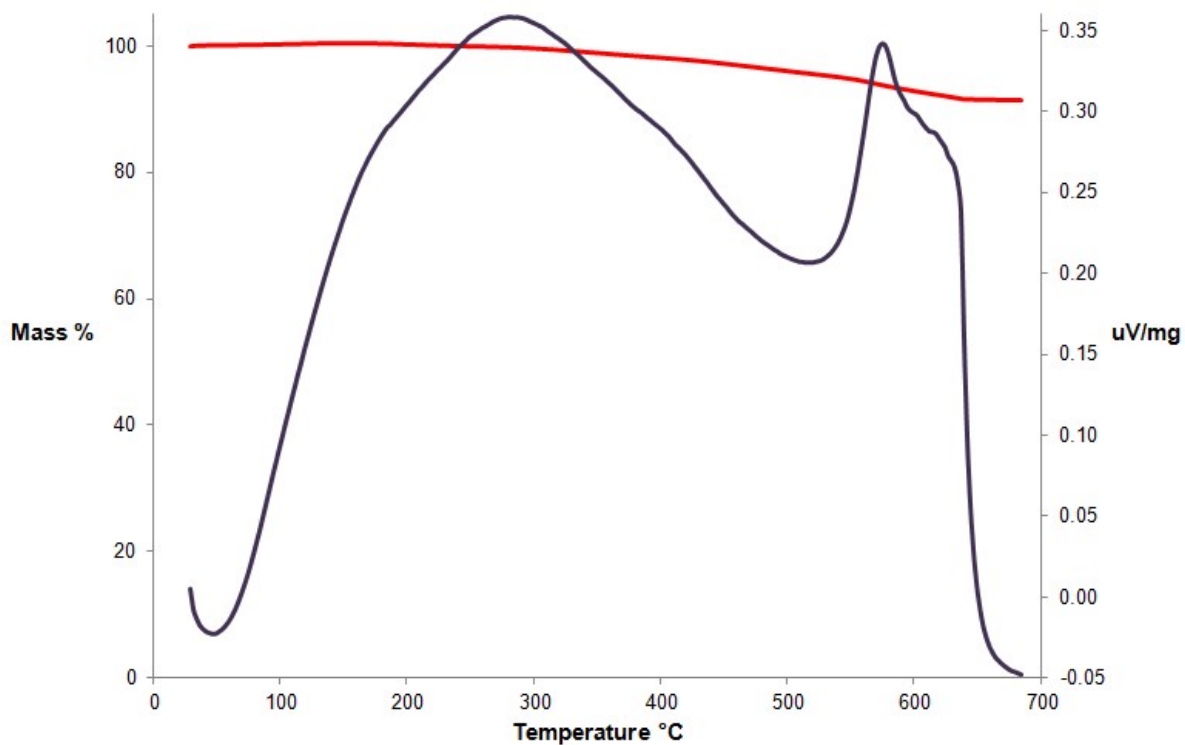


Figure S13. TGA (red) and DTA (purple) curves of Cr-25C-H₂

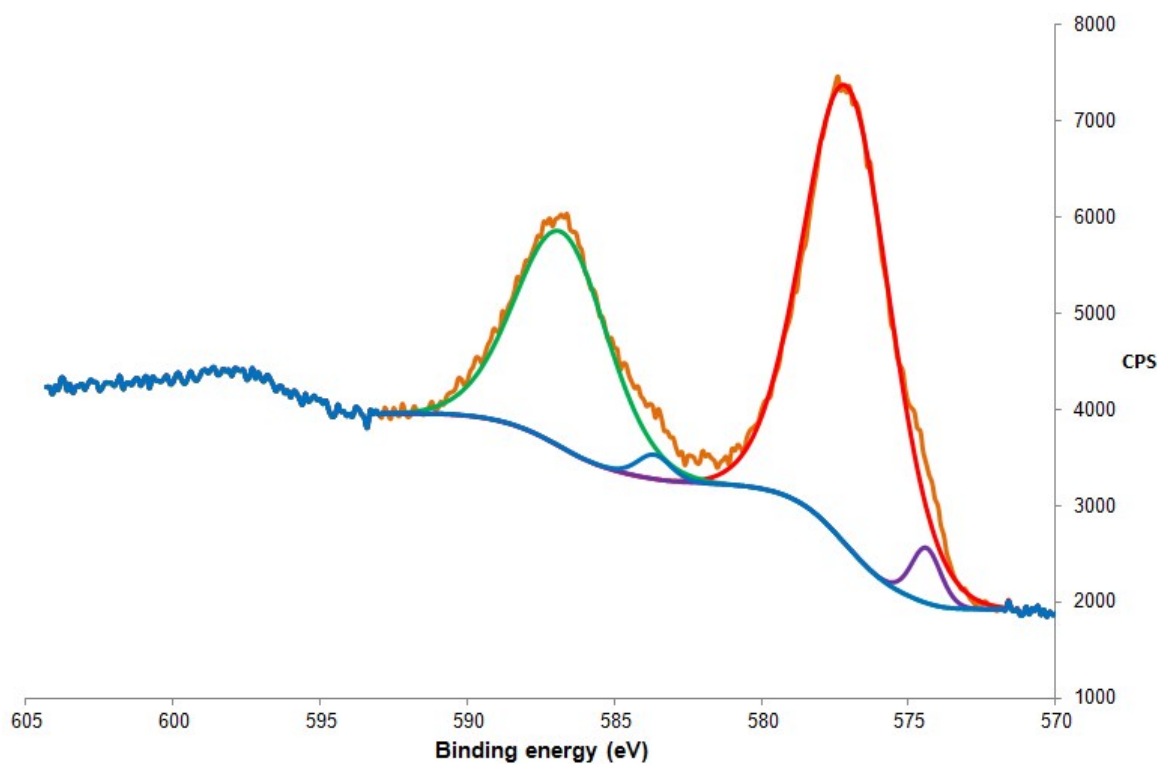


Figure S14. Peak fitting of chromium 2p_{1/2} and 2p_{3/2} region of XPS of Cr-100

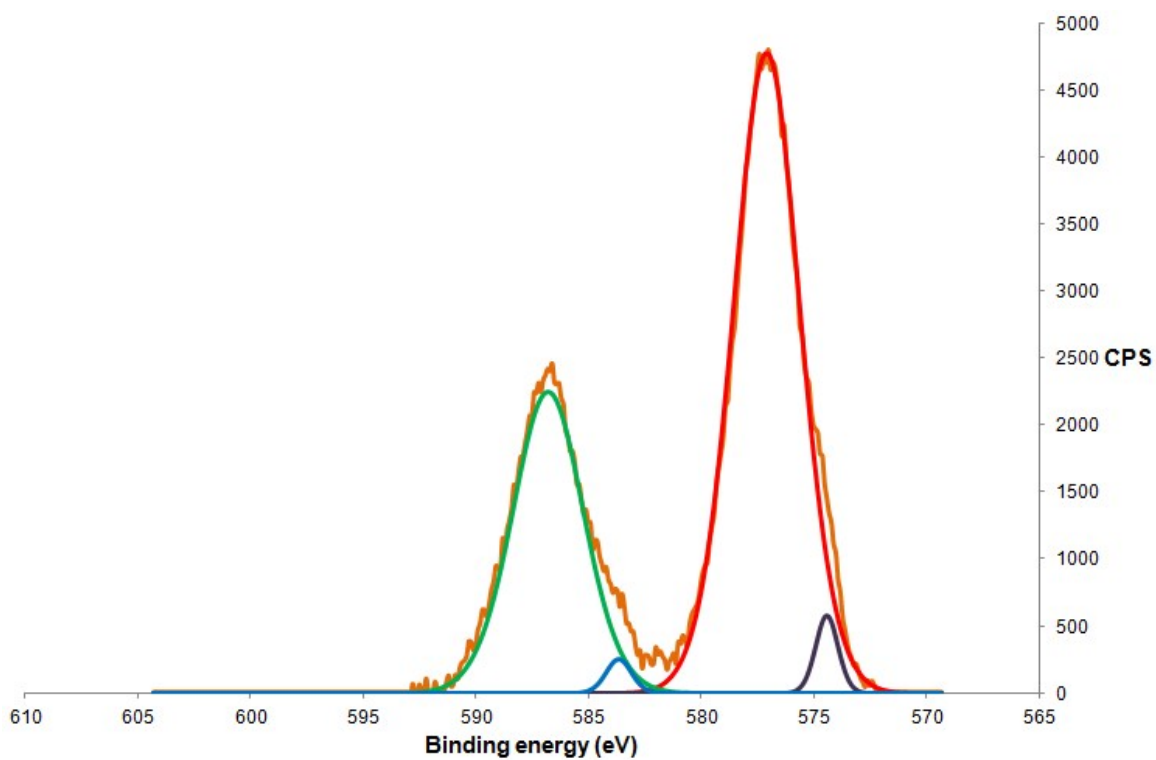


Figure S15. Baseline corrected peak fitting of chromium 2p_{1/2} and 2p_{3/2} region of XPS of Cr-100

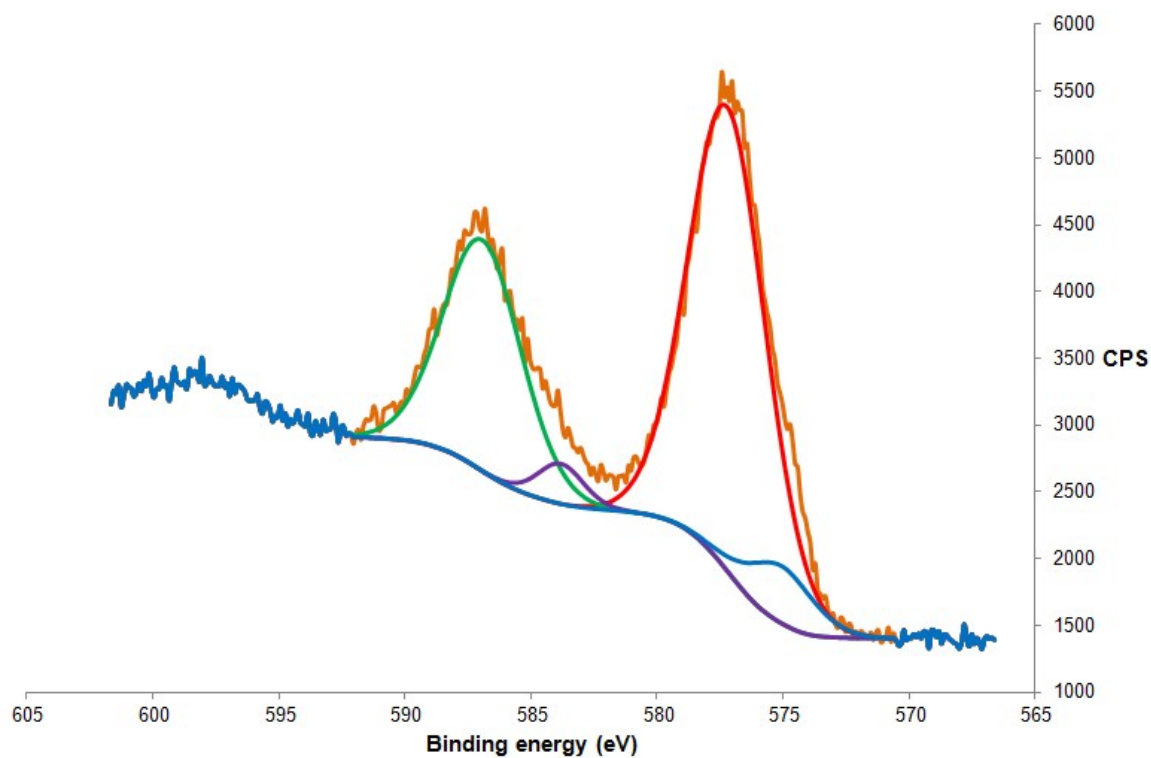


Figure S16. Peak fitting of chromium $2p_{1/2}$ and $2p_{3/2}$ region of XPS of Cr-150C-H₂

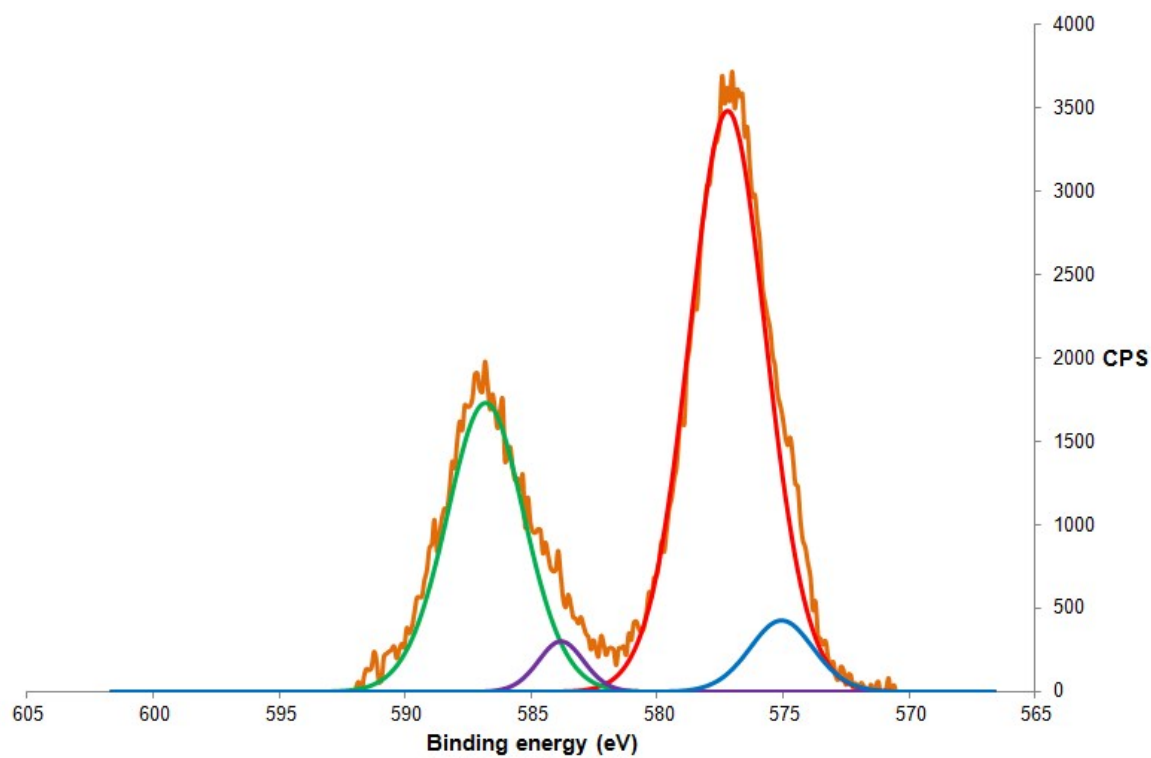


Figure S17. Peak fitting of chromium $2p_{1/2}$ and $2p_{3/2}$ region of XPS of Cr-150C-H₂

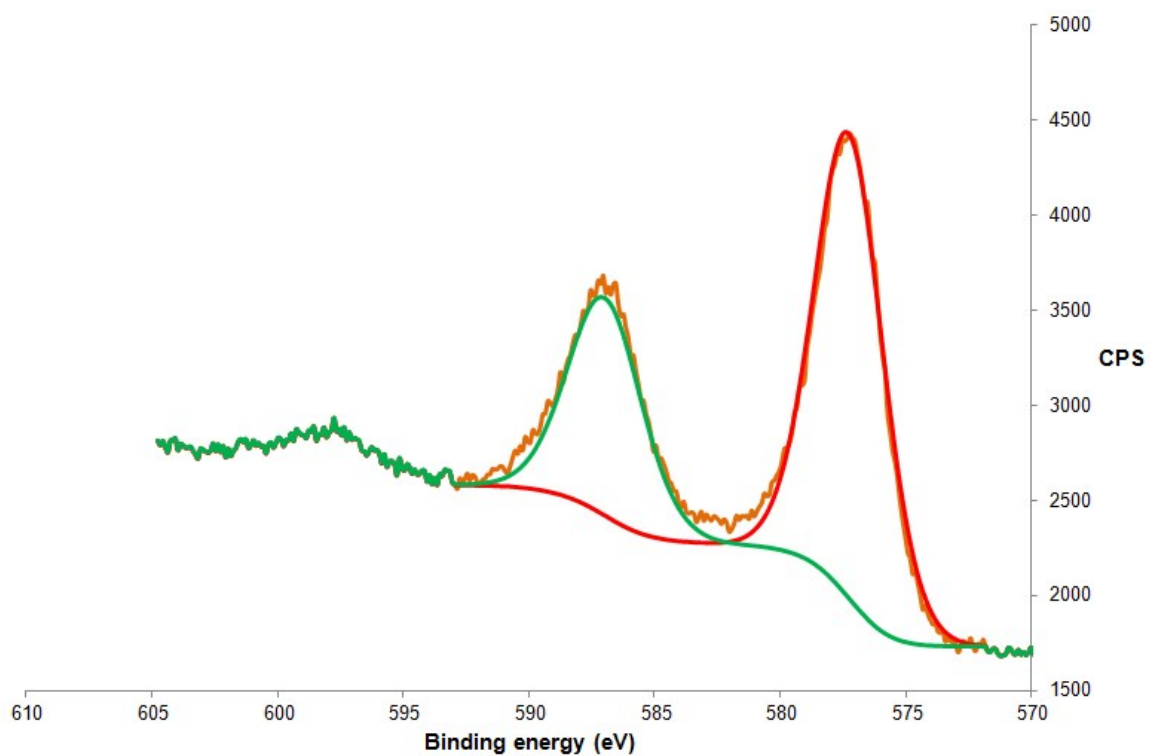


Figure S18. Peak fitting of chromium 2p_{1/2} and 2p_{3/2} region of XPS of Cr-25C-H₂

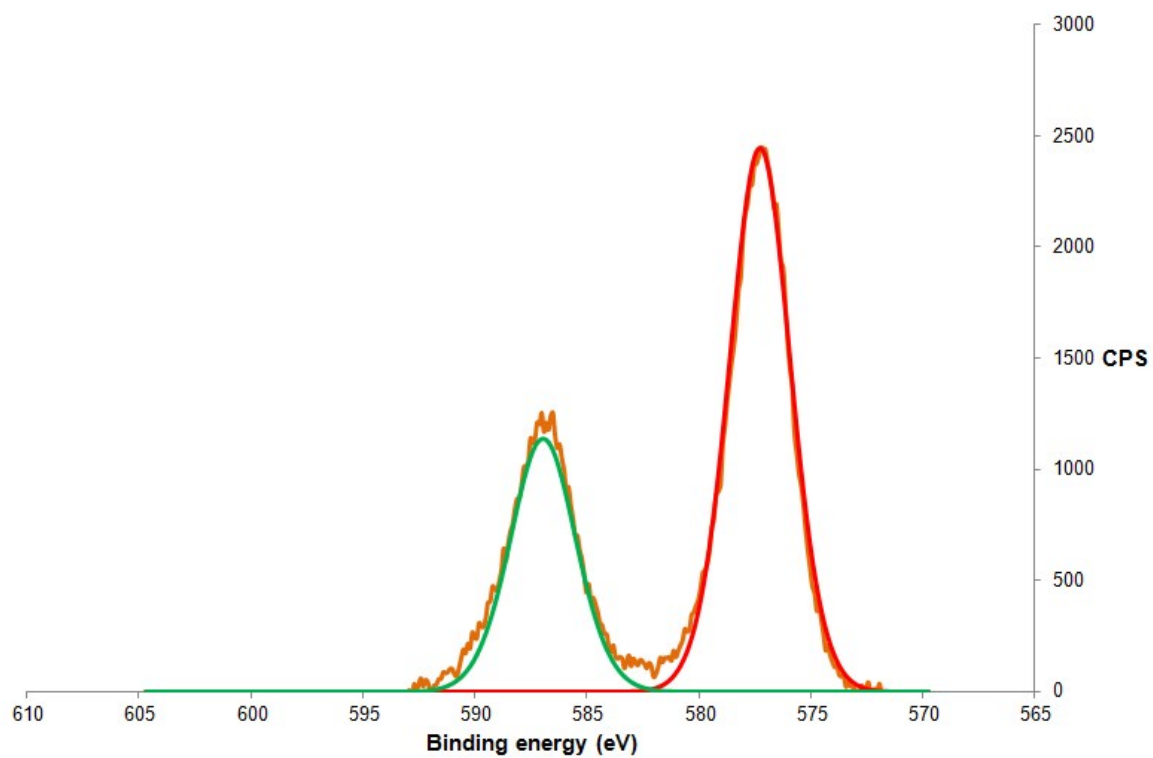


Figure S19. Baseline corrected peak fitting of chromium 2p_{1/2} and 2p_{3/2} region of XPS of Cr-25C-H₂